Supporting Information

Mintz *et al.* 10.1073/pnas.0807543105

SI Text

Cell Surface and Membrane Localization. DU145 cells were labeled with membrane impenetrable Biotin-LC-LC-NHS EZ link (Pierce). The biotinylated membrane proteins were washed, solubilized, and clarified followed by IP with streptavidin. Membrane fractionation was performed as described (1). Confocal images were acquired on an LSM 510 (Zeiss) confocal microscope. DU145 cells were grown on fibronectin-coated slides, fixed with 4% paraformaldehyde (PFA) and labeled with the appropriate antibodies (polyclonal CRKL antibody and monoclonal AHSG antibody). The electron microscopy images (SEM and TEM) were acquired on JSM 5900 scanning or JEM 1010 transmission electron microscope (JEOL). Gold nanoparticle antibody conjugates were prepared by mixing 20- to 25-nm or 40- to 45-nm gold in sodium borate and verified by TEM. DU145 cells were labeled on ice with appropriate antibodies (monoclonal anti-CRKL, anti-β_1 integrin, and anti-AHSG antibodies), followed by secondary conjugated-fluorescent antibodies, and were analyzed by FACS.

Design of Mutant Proteins and Scrambled and Mutant Tumor-Homing Phage. The ORF of full-length CRKL cDNA (Invitrogen) was amplified by PCR and cloned into pET28a (Novagen). cDNAs corresponding to each of the SH domains were amplified by PCR and cloned into the SacI and XhoI restriction sites of the vector. Constructs were verified by restriction digestion and DNA sequencing and transfected into BL21 cells (Stratagene); recombinant proteins were purified on His-tag columns (Qiagen). Purified recombinant proteins were verified through Coomassie blue staining and Western blot analysis with anti-CRKL and anti-His antibodies. To show that the CRKL protein oligomerizes, we incubated increasing concentrations of recombinant GST-CRKL with immobilized CRKL protein (His tag recombinant form) or immobilized BSA overnight at 4 °C, followed by 3 washes. Protein interactions were detected with an antibody against GST.

We designed and constructed phage displaying scrambled peptide sequences and mutants (Pro → Ala and Phe-Phe-Trp → Ala-Ala-Ala) from the selected CRKL binding tumor homing phage peptide YRCTLNSPFFWEDMTHECHA. Scrambled peptide sequences (YRFCTSPFHEWHLENTDMCA, YRECTDSPHEFHLWNTMCAF, YRCETDSPHEFHLWNTMCAF, YRCETDSPHEFHLWNTFCAM), mutants (YRCTLNSAFFWEDMTHECHA and YRCTLNSPAAAEDMTHECHA), or native PSI-derived phage (CNSTFLQEGMPTSAC) were cloned into the SfiI-digested fUSE5 vectors (2). Briefly, synthetic oligonucleotides (500 ng) were converted to dsDNA by PCR with the primer set 5′-GTGAGCCGGCTGCCC-3′ and 5′-TTCGGCCCCAGCGGC-3′ (Sigma–Genosys) and 2.5 units of Taq-DNA polymerase (Promega). Oligonucleotides were digested with BglI and ligated into an SfiI-digested fUSE5 vector.

Peptide Binding and Internalization Assays. The following recombinant His tag proteins were added to the coated plates: rCRKL, rCRKL-SH2 domain, rCRKL-SH3 (N) domain, and rCRKL-SH3 (C) domain. An unrelated control protein (α_2-Heremans-Schmid glycoprotein; AHSG) served as a negative control.

The conjugated tumor-homing peptide YRCTLNSPFFWEDMTHECHA-GG-$_D$(KLAKLAK)$_2$ or the untargeted control peptide $_D$(KLAKLAK)$_2$ was synthesized, and increasing equimolar peptide concentrations were added to the DU145 cells. Cell viability was assayed by the WST-1 reagent (Roche) and annexin-V staining for apoptosis (3, 4). For tumor-homing phage localization studies, cells were incubated with 10^9 transducing units (TU) of the tumor-homing or a negative control phage for 6 and 24 h. Wells were washed with 20 mM glycine to remove nonspecific cell surface-bound phage and were subsequently fixed with 4% PFA. The nonpermeabilized cells were incubated with rabbit anti-fd bacteriophage antibody (Sigma) for 2 h at room temperature followed by 1-h incubation with Cy3-labebled anti-rabbit IgG antibody (Jackson ImmunoResearch). Cells were again fixed with 4% PFA and mounted in the presence of DAPI (Vector Laboratories), and images were acquired with an Olympus fluorescence microscope.

Phage Binding and Protein–Protein Assays. Recombinant proteins were coated on microtiter wells as described (2). Briefly, proteins (50 μL of 1 μg/mL in PBS) were immobilized on microtiter wells overnight at 4 °C. Wells were washed twice with PBS, blocked with PBS containing 3% BSA for 2 h at room temperature, and incubated with 10^9 TU of wild-type tumor-homing phage, scrambled phage (YRFCTSPFHEWHLENTDMCA, YRECTDSPHEFHLWNTMCAF, YRCETDSPHEFHLWNTMCAF, YRCETDSPHEFHLWNTFCAM), mutant phage (YRCTLNSAFFWEDMTHECHA, YRCTLNSPAAAEDMTHECHA), PSI-derived cyclic phage (CNSTFLQEGMPTSAC), or fd-tet phage in 50 μL of PBS containing 1.5% BSA. After 1 h at room temperature, wells were washed 10 times with PBS, and phage were recovered by bacterial infection. ELISA with polyclonal anti-CKRL confirmed the presence and concentration of the CKRL recombinant proteins on the wells. To test the binding of the tumor-homing phage to SH3-containing proteins, we coated microtiter wells at 4 °C overnight with 250 ng/mL of recombinant GST-SH3 domains (CKRL-D1, CKRL-D2, grb2-D1, grb2-D2, Lyn, src; Pronomics), rCKRL protein, and the negative controls GST or BSA. For the SH3 (C) mutant binding studies, 2 μg/mL of His tag recombinant wild-type SH3-C and mutant SH3 (C) domains were coated. The tumor-homing phage (10^{10} TU) or fd-tet phage was added to each well, and the binding assay was preformed. Protein interaction experiments between CRKL and integrin β_1 were done on wells coated with $\alpha5\beta_1$, $\alpha v\beta_3$ or $\alpha v\beta_5$ integrins (Chemicon) at 1 μg per well. To evaluate the inhibitory binding of CKRL to the β_1 integrin by GST-PSI, we preincubated CKRL and increasing concentrations of GST-PSI or GST for 15 min at room temperature before their addition to the coated wells. After 3 h, binding of CKRL to integrins was detected with an anti-CKRL antibody followed by an HRP-conjugated anti-rabbit IgG. To confirm that equal amounts of the integrins were bound to the plates, we performed parallel experiments with a 1:1,500 dilution of an anti-integrin antibody (Amersham Pharmacia).

In Vivo Tumor Targeting and Inhibition. We used male nude mice bearing human DU145 xenografts or female nude mice with human KS1767-derived xenografts s.c. and immunocompetent BALB/c female mice bearing EF43-*FGF4*-derived breast tumors orthotopically in the mammary fat pad. Briefly, mice bearing tumors (≈8 mm) were anesthetized and received 5×10^{10} TU (tail vein) of wild-type YRCTLNSPFFWEDMTHECHA-phage, or negative controls: fd-tet phage, scrambled phage, or mutant phage (see above for sequences). Cohorts of mice with size-matched tumors received each set of phage clones. After 24 h, tumors were dissected, and phage recovered by bacterial

infection were normalized to weight. The experiments were repeated twice for each tumor model. For the inhibition of tumor targeting, the CRKL-homing phage was incubated with the recombinant GST-CRKL or control GST protein for 30 min at 37 °C and was subsequently administered i.v. into prostate tumor-bearing mice.

1. Mintz PJ, *et al.* (2003) Fingerprinting the circulating repertoire of antibodies from cancer patients. *Nat Biotechnol* 21:57–63.
2. Smith GP, Scott JK (1993) Libraries of peptides and proteins displayed on filamentous phage. *Methods Enzymol* 217:228–257.
3. Zurita AJ, *et al.* (2004) Combinatorial screenings in patients: The interleukin-11 receptor α as a candidate target in the progression of human prostate cancer. *Cancer Res* 64:435–439.
4. Marchiò S, *et al.* (2004) Aminopeptidase A is a functional target in angiogenic blood vessels. *Cancer Cell* 5:151–162.

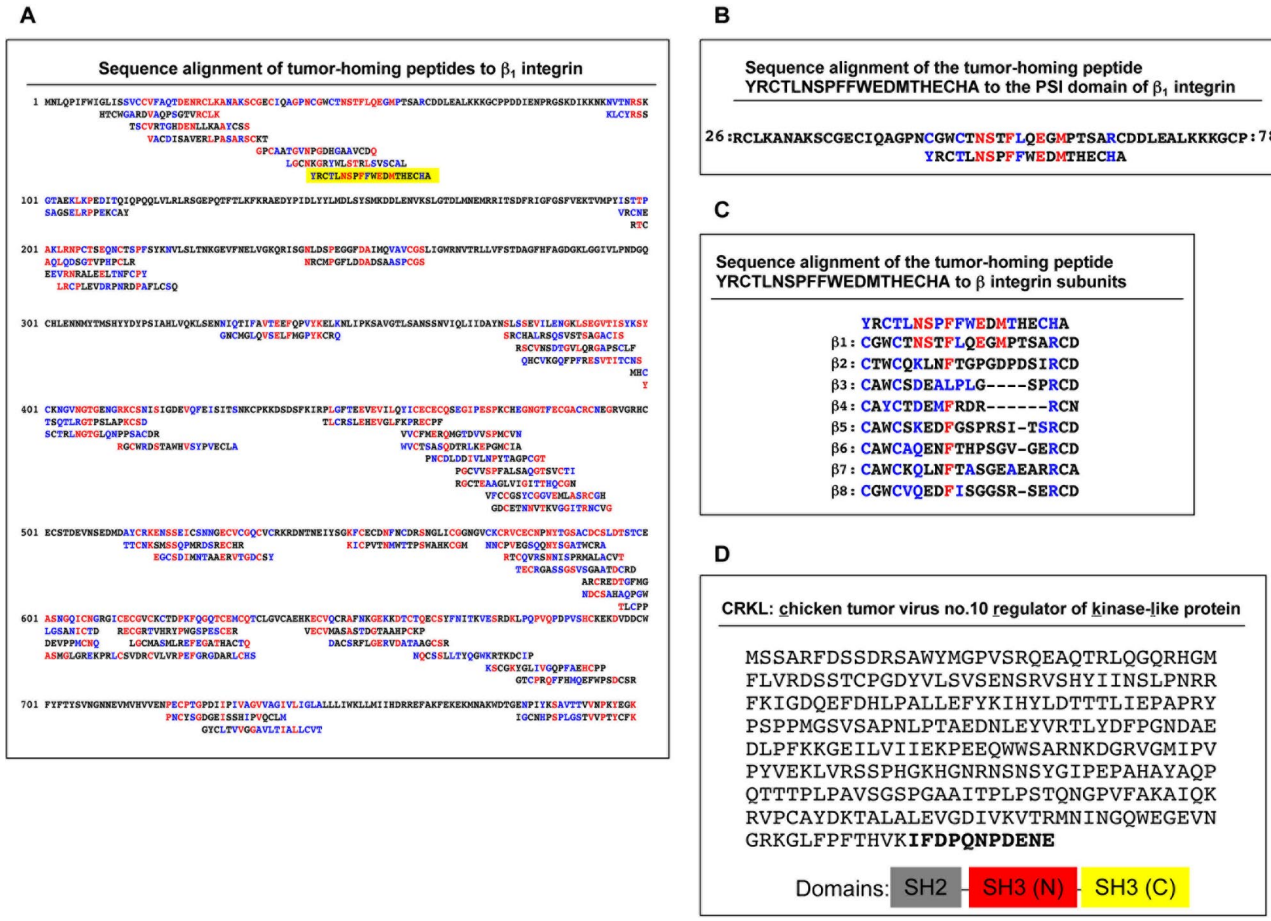

Fig. S1. Sequence alignment of tumor-homing peptides, β_1 Integrin and CRKL. (*A*) Sequence alignment of all tumor homing peptides and β_1 integrin. Similarities between residues are depicted in blue, and 100% identity is depicted in red. (*B*) The tumor-homing peptide YRCTLNSPFFWEDMTHECHA matches to the PSI domain (sequence region 26–78 residues). (*C*) Sequence alignment of all eight β integrin-subunits and the YRCTLNSPFFWEDMTHECHA peptide sequence. (*D*) Identification of CRKL by mass spectrometry. A peptide sequence (in bold) was obtained by mass spectrometry that matched 100% to CRKL by BLAST homology search (accession no. NP005198). CRKL is composed of three domains: SH2, SH3 (N, amino-terminal), and SH3 (C, carboxyl-terminal).

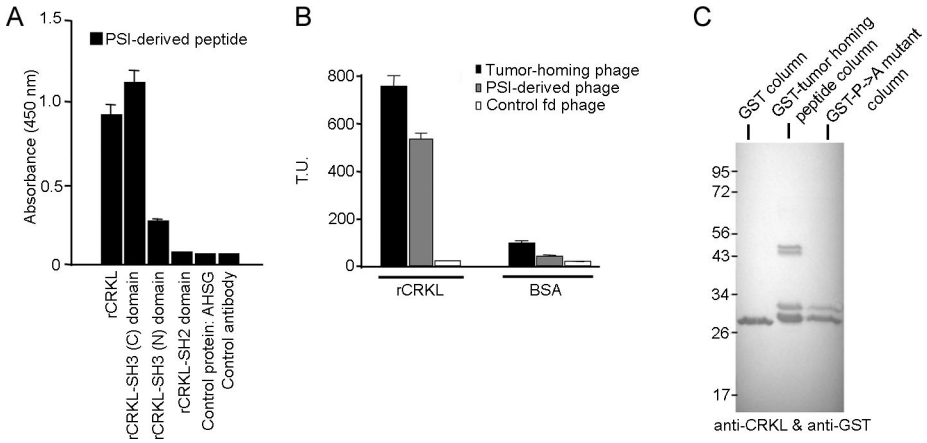

Fig. S2. The tumor-homing peptide specifically binds to CRKL. (*A*) The recombinant His-tag rCRKL, rCRKL-SH3 (N) domain, and rCRKL-SH3 (*C*) domain bind to the synthetic peptide NSTFLQEGMPTSA corresponding to a region in the PSI domain. $P < 0.001$ vs. controls (Student's *t* test). (*B*) Tumor-homing phage (displaying YRCTLNSPFFWEDMTHECHA) and the PSI-derived phage (displaying CNSTFLQEGMPTSAC) bind to recombinant CRKL. Bars represent mean ± SD from triplicate wells. $P < 0.001$ vs. fd phage (Student's *t* test). (*C*) Affinity purification of CRKL from serum-free conditioned medium. A column containing the recombinant GST-tag fusion protein of the tumor-homing peptide binds CRKL from the serum-free conditioned medium, but a control peptide column containing a single point mutation (Pro→Ala) does not.

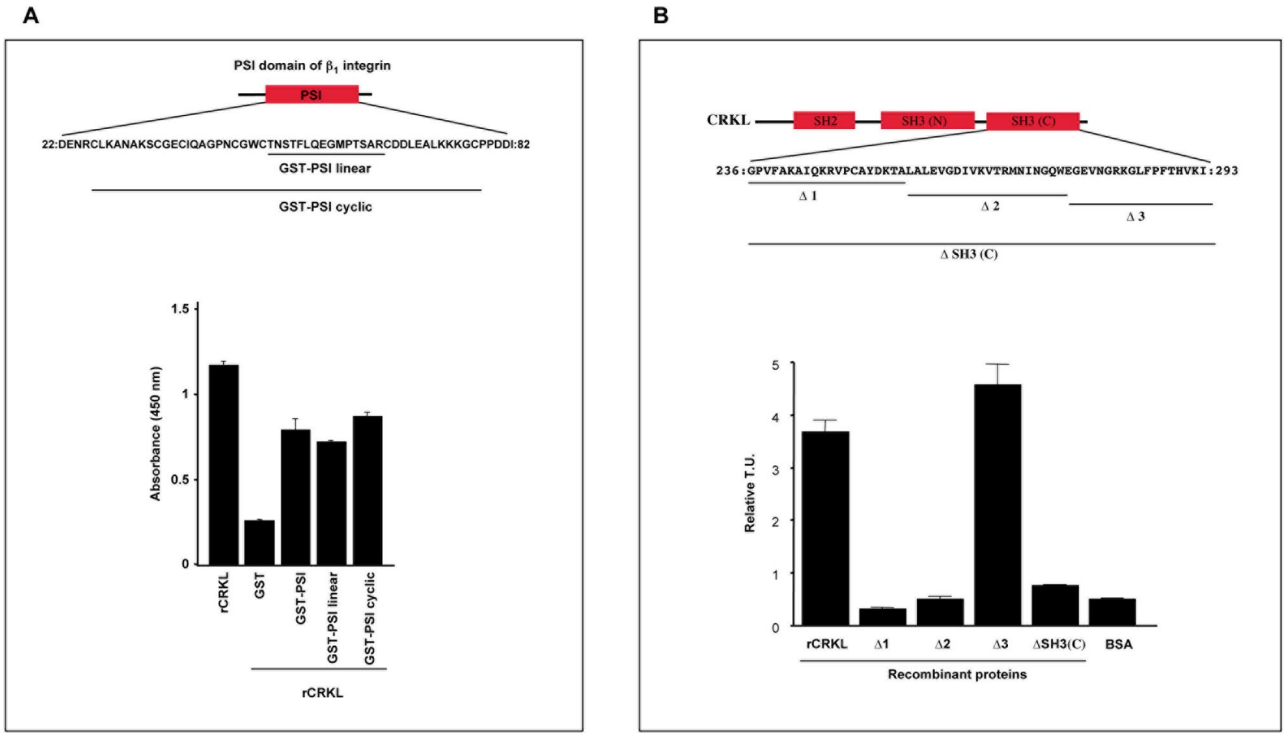

Fig. S3. Sequence requirements for the binding of the PSI and SH3 (C) domains to CRKL. (*A*) (*Upper*) Scheme of the PSI-derived region of β_1 integrin. (*Lower*) Recombinant GST fusion protein of the entire PSI domain (residues 22–82), GST-PSI linear (residues 48–62), and GST-PSI cyclic (residues 26–74) were produced for binding assays. Both the linear and the cyclic PSI-derived regions bind to CRKL. (*B*) (*Upper*) Scheme of the CRKL SH3 (C) domain and the control deletion mutants generated as His-tag recombinant proteins. Four mutants were generated and tested: Δ1 (deleted residues 236–256), Δ2 (deleted residues 257–277), Δ3 (deleted residues 278–293), and ΔSH3 (C) (deleted residues 236–293). (*Lower*) The binding region is located between residues 236 and 277 of the SH3 (C) domain.

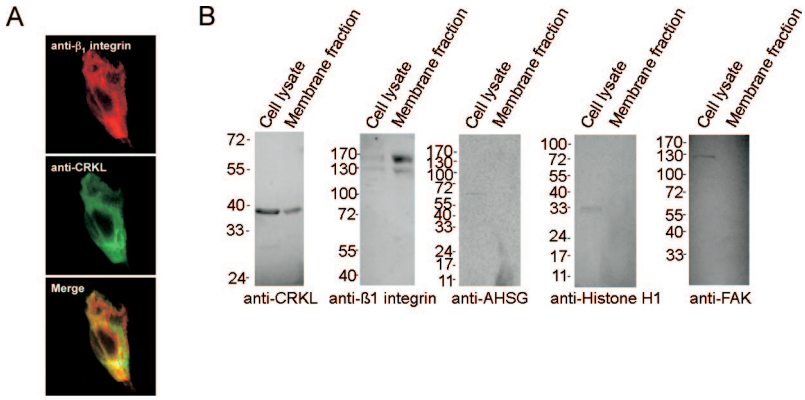

Fig. S4. Immunofluorescence and membrane fractionation confirm CRKL localization at the cell surface. (*A*) Immunofluorescence localization of CRKL on fixed DU145 cells by confocal microscopy. (*B*) CRKL is present in DU145 membrane fractions and cell lysates. An anti-CRKL polyclonal antibody was used in study. (Magnification: ×600).

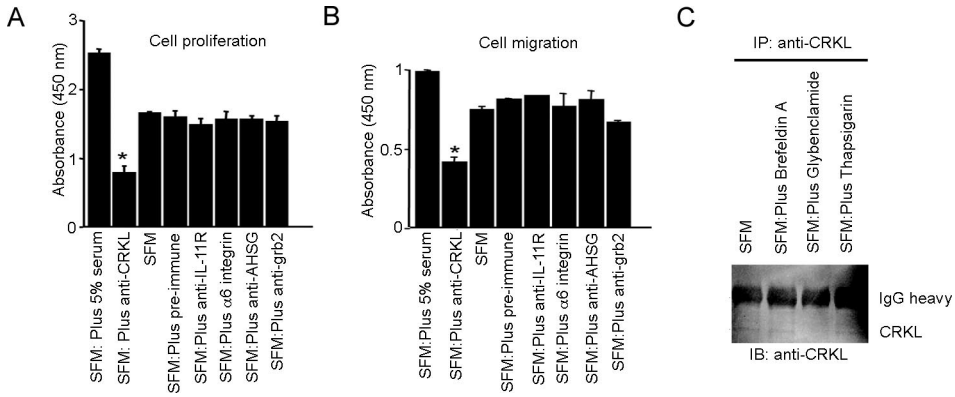

Fig. S5. Neutralization of CRKL function and release inhibits cell proliferation and migration. (*A* and *B*) CRKL antibody neutralizes the extracellular form of CRKL in the medium and affects cell proliferation and migration. Control antibodies were: anti-IL11 receptor, anti-AHSG, anti-grb2, anti-α_6 integrin, and preimmune antibodies. Bars represent mean $\pm$ SD from duplicate wells. $*$, $P < 0.01$ vs. SFM. (*C*) Classical export inhibitors (brefeldin A and thapsigargin) do not prevent CRKL secretion, whereas the ABC-transporter inhibitor, glybenclamide, prevents CRKL transfer to the extracellular compartment. All inhibitors used at 0.4mM.

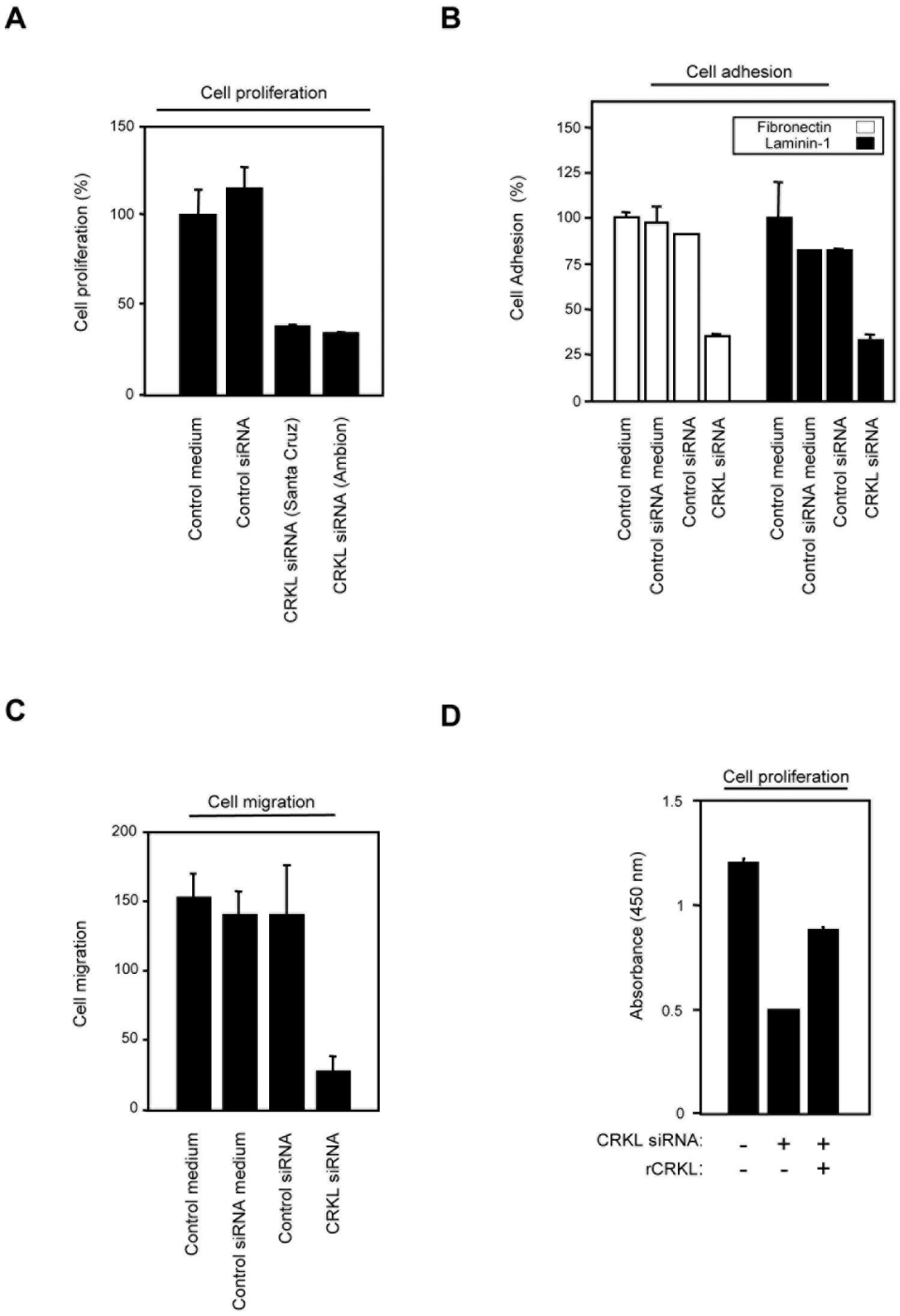

Fig. S6. Effects of CRKL siRNA silencing. Cell proliferation (*A*), adhesion (*B*), and migration (*C*) are shown. Standard deviations of the mean from triplicate wells are shown. (*D*) DU145 cells were transfected with CRKL siRNA for 48 h before exogenously adding recombinant CRKL to the wells. Cell proliferation was determined with the WST-1 reagent.

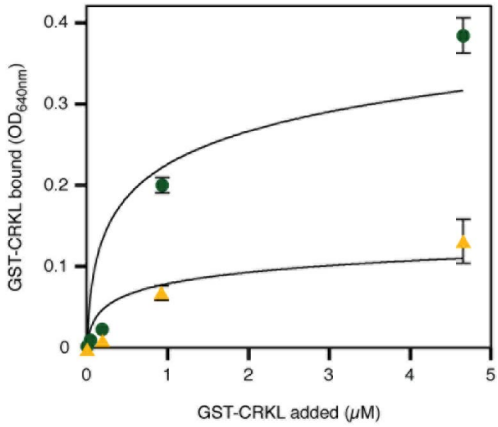

Fig. S7. CRKL oligomerization. Increasing concentrations of recombinant GST-CRKL were incubated with immobilized CRKL protein (His tag recombinant form) or immobilized BSA. The binding was evaluated by ELISA with an antibody against GST.

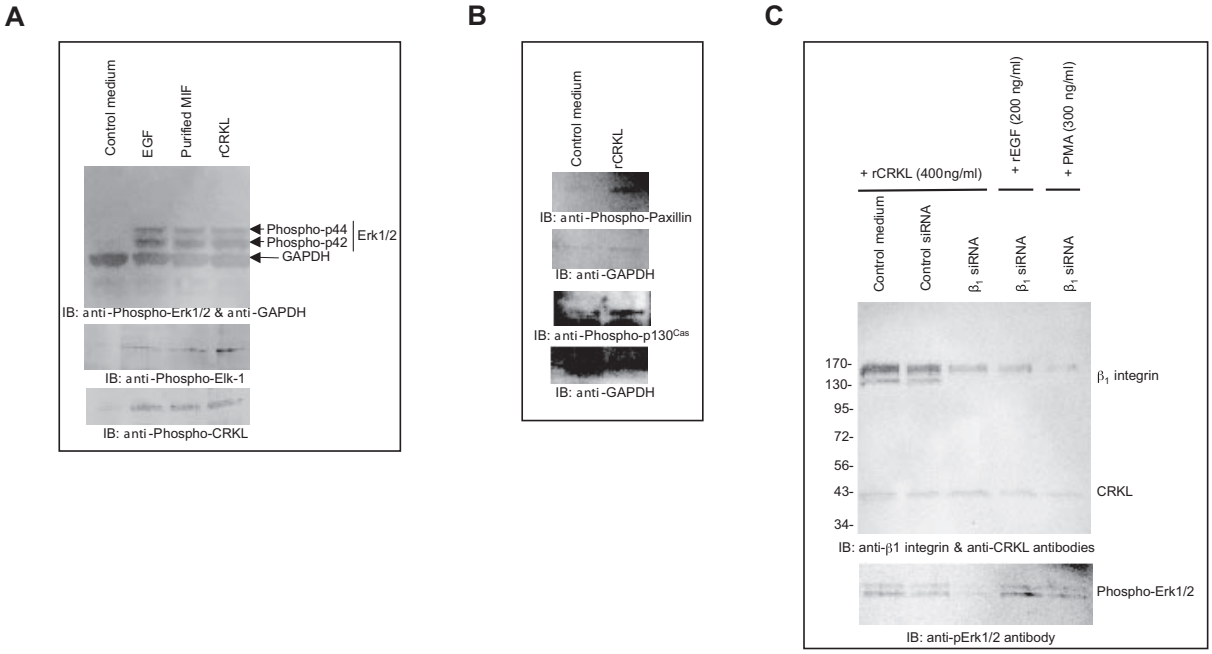

Fig. S8. CRKL signaling through the MAPK and integrin-mediated pathways. (*A* and *B*) Activation of the MAPK and integrin-mediated pathways by exogenous recombinant CRKL protein (400 ng/ml). Recombinant epidermal growth factor (EGF) at 200 ng/mL, purified macrophage migration inhibitory factor (MIF) at 300 ng/mL, and phorbol myristate acetate (PMA) served as positive controls. (*C*) Exogenous rCRKL does not stimulate the ERK pathway in ß1 integrin siRNA-silenced cells.

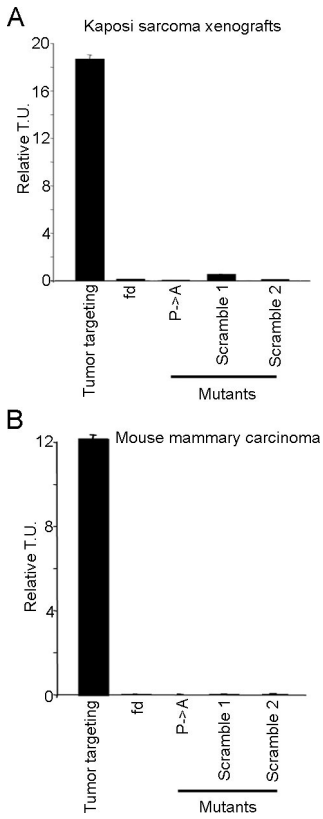

Fig. S9. Tumor targeting. (*A* and *B*) In vivo homing of targeted or control phage constructs in mice bearing different tumor types. Tumor-homing phage localized to tumors preferentially compared with controls. Representative data from 2 independent experiments are shown. Bars represent mean ± SD. Tumor targeting, YRCTLNSPFFWEDMTHECHA; fd, fd-tet phage (negative control); P→A, YRCTLNSAFFWEDMTHECHA; Scramble 1, YRFCTSPFHEWHLENTDMCA; Scramble 2, YRECTDSPHEFHLWNTMCAF (bold indicates residue mutations).

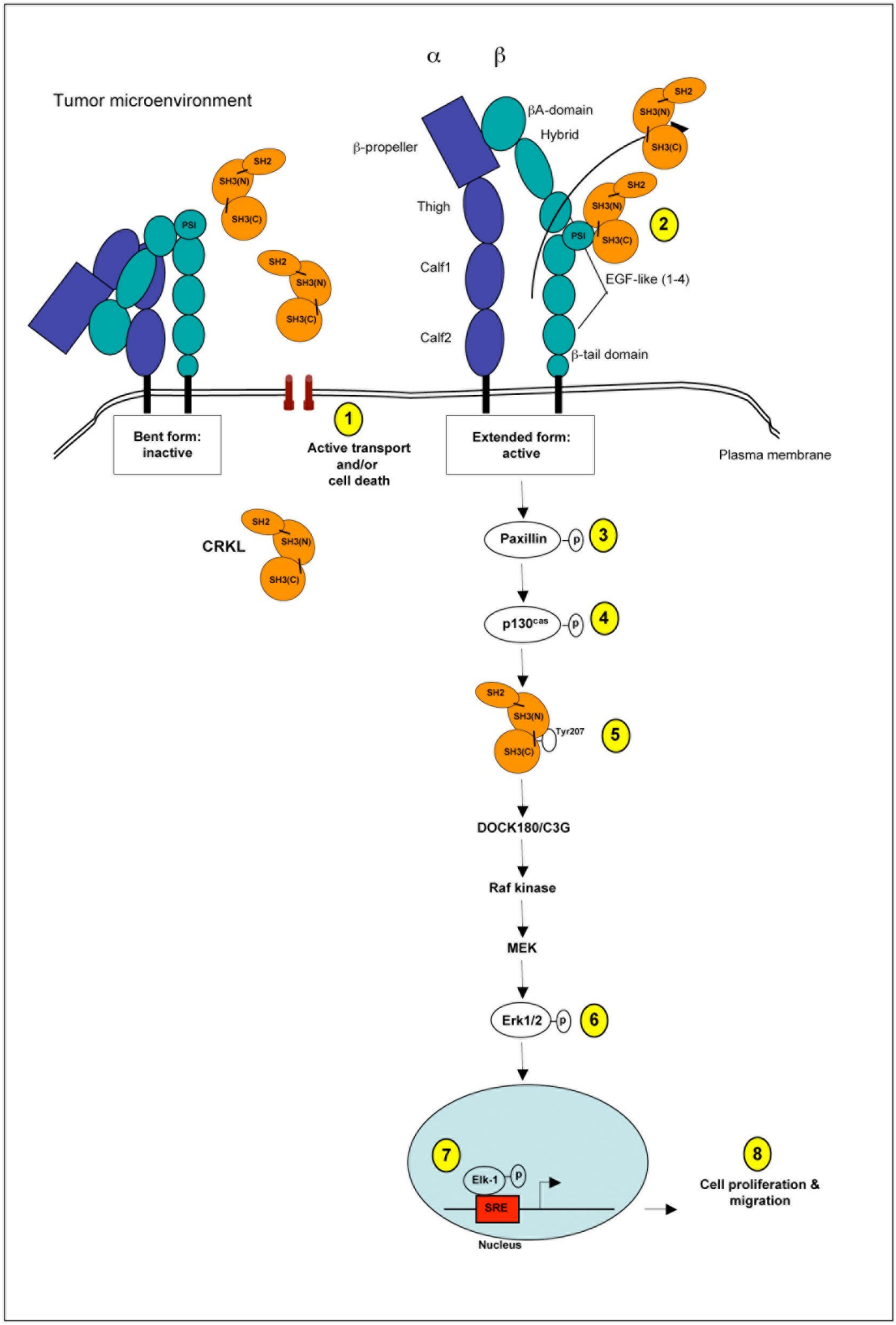

Fig. S10. A working model based on the switchblade integrin activation. A hypothetical pathway used by extracellular (secreted and/or released) CRKL to activate the integrin-mediated MAPK cascade to promote cell proliferation and migration is shown.

Table S1. PCR primer sets

Primer	Sequence
Full-length CRKL	5′-CACAGAGCTCAACACCATGTCCTCCGCCAGGTTCG-3′
	5′-CACACTCGAGCTCGTTTTCATCTGGGTTTTGAGGG-3′
CRKL SH2 domain	5′-CACAGAGCTCGCCACCATGTCCTCCGCCAGGTTCGACTCCT-3′
	5′-CACACTCGAGTTCCAGGTTATCTTCTGCTGTAGGC-3′
CRKL SH3 (N) domain	5′-CACAGAGCTCGCCACCATGGGATCTGTCTCAGCACCCAACC-3′
	5′-CACACTCGAGATTCTGTGTGGATGGCAAAGGGGTG-3′
CRKL SH3 (C) domain	5′ CACAGAGCTCGCCACCATGAGATCCTCACCACACGGAAAGCATG-3′
	5′ CACACTCGAGGTTTTCATCTGGGTTTTGAGGGTC-3′
CRKL-SH3-Δ1	5′-CACCCCTTTGCCATCCACACAGAATTTGGCATTAGAGGTTGGTGACATCG-3′
	5′ CGATGTCACCAACCTCTAATGCCAAATTCTGTGTGGATGGCAAAGGGGTG-3′
CRKL-SH3-Δ2	5′ CCCTGTGCTTATGACAAGACTGCCGAAGGCGAAGTGAACGGGCGCAAA-3′
	5′ TTTGCGCCCGTTCACTTCGCCTTCGGCAGTCTTGTCATAAGCACAGGG-3′
CRKL-SH3-Δ3	5′-CAAGGATGAATATAAATGGCCAGTGGTTTGACCCTCAAAACCCAGATGAAAACG-3′
	5′-CGTTTTCATCTGGGTTTTGAGGGTCAAACCACTGGCCATTTATATTCATCCTTG-3′
CRKL-SH3-Δ	5′-CACCCCTTTGCCATCCACACAGAATTTTGACCCTCAAAACCCAGATGAAAACG-3′
	5′CGTTTTCATCTGGGTTTTGAGGGTCAAAATTCTGTGTGGATGGCAAAGGGGTG-3′
PSI domain	5′-CACAGAGCTCGCCACCATGAATTTACAACCAATTTTCTGG-3′
	5′-CACACTCGAGTGTTCCTTTGCTACGGTTGGTTAC-3′
PSI linear form	5′-CATGGGCGAATTCACAAATTCAACATTTTTACAGGAAGGAATGCCTACTTCTGCACGAC-3′
	5′-TCGAGTCGTGCAGAAGTAGGCATTCCTTCCTGTAAAAATGTTGAATTTGTGAATTCGCC-3′
PSI cyclic form	5′-CACACCATGGGCGAATTCTGTTTAAAAGCAAATGCCAAATCATG-3′
	5′-CACACTCGAGGCAACCCTTCTTTTTTAAGGCTTC-3′

Table S2. siRNA oligonucleotides

Oligonucleotide	Sequence
Santa Cruz, CRKL	GUCGUAUUGUCAAAGAGUATT
	GUAGCAGACAACACACAAATT
	CAGCAGACCUAGAAAUGUATT
Dharmacon, CRKL	CCGAAGACCUGCCCUUUAAUU
	GAAGAUAACCUGGAAUAUGUU
	GUCACAAGGAUGAAUAUAAUU
	AAUAGGAAUUCCAACAGUUUU
Ambion, CRKL	GGUAUCCAAGCCCACCAAUTT
	GGAUGAAUAUAAAUGGCCATT
Santa Cruz, β_1 integrin	GAGAUGAGGUUCAAUUUGATT
	GAUGAGGUUCAAUUUGAAATT
	GUACAGAUCCGAAGUUUCATT
Dharmacon, control	AUGAACGUGAAUUGCUCAAUU